

# The effect of sampling rate and anti-aliasing filters on high-frequency response spectra

David M. Boore · Christine A. Goulet

Received: 6 November 2013 / Accepted: 11 December 2013 / Published online: 25 December 2013  
© Springer Science+Business Media Dordrecht (outside the USA) 2013

**Abstract** The most commonly used intensity measure in ground-motion prediction equations is the pseudo-absolute response spectral acceleration (PSA), for response periods from 0.01 to 10 s (or frequencies from 0.1 to 100 Hz). PSAs are often derived from recorded ground motions, and these motions are usually filtered to remove high and low frequencies before the PSAs are computed. In this article we are only concerned with the removal of high frequencies. In modern digital recordings, this filtering corresponds at least to an anti-aliasing filter applied before conversion to digital values. Additional high-cut filtering is sometimes applied both to digital and to analog records to reduce high-frequency noise. Potential errors on the short-period (high-frequency) response spectral values are expected if the true ground motion has significant energy at frequencies above that of the anti-aliasing filter. This is especially important for areas where the instrumental sample rate and the associated anti-aliasing filter corner frequency (above which significant energy in the time series is removed) are low relative to the frequencies contained in the true ground motions. A ground-motion simulation study was conducted to investigate these effects and to develop guidance for defining the usable bandwidth for high-frequency PSA. The primary conclusion is that if the ratio of the maximum Fourier acceleration spectrum (FAS) to the FAS at a frequency  $f_{saa}$  corresponding to the start of the anti-aliasing filter is more than about 10, then PSA for frequencies above  $f_{saa}$  should be little affected by the recording process, because the ground-motion frequencies that control the response spectra will be less than  $f_{saa}$ . A second topic of this article concerns the resampling of the digital acceleration time series to a higher sample rate often used in the computation of short-period PSA. We confirm previous findings that sinc-function interpolation is preferred to the standard practice of using linear time interpolation for the resampling.

---

D. M. Boore (✉)  
U. S. Geological Survey, Menlo Park, CA, USA  
e-mail: boore@usgs.gov

C. A. Goulet  
Pacific Earthquake Engineering Research Center, Berkeley, CA, USA

**Keywords** Engineering seismology · Strong motion · Record processing · Response spectra · Earthquake engineering · Anti-aliasing filter

## 1 Introduction

High-frequency pseudo-absolute response spectral accelerations (PSAs) are often needed in the design of stiff structures and equipment within those structures, nuclear power plants being a prime example. If natural processes have removed enough high-frequency energy from the ground motions, as is often the case in tectonically active regions, the response spectra can be computed to arbitrarily high frequencies, regardless of the sample rate of the data or the high-cut filters used in processing the data (Douglas and Boore 2011). This is so because the response of a high-frequency oscillator will be controlled by ground motions at frequencies much lower than the oscillator frequency. This may not be true, however, for records for which the natural attenuation of motion has not decreased the Fourier spectral content significantly for frequencies at which the anti-aliasing filter used in modern digital records begins to remove the high-frequency content. For example, ground motions in the central and eastern North America region (CENA) often contain a significant amount of energy at frequencies exceeding 10 Hz, both because the records are from very hard rock sites and because the anelastic attenuation is fairly low. More than 70 % of the time series initially collected for the NGA-East (Next Generation Attenuation for CENA) database came from instruments with a sample rate of 40 sps (samples per second) or less, with an anti-aliasing filter that removes the energy above 20 Hz (or lower, depending on the original sampling rate). For this reason, there is the possibility that the response spectra from such records are not trustworthy at frequencies of importance to stiff structures (Silva and Darragh 1995). To investigate this, we use a simulation study in which ground accelerations are generated at a high sample rate for a number of magnitudes, distances, and  $\kappa_0$  values [the parameter that controls distance-independent decay of high-frequency ground motion; see Anderson and Hough (1984)]. This approach was also followed by Douglas and Boore (2011), who were concerned with the effect of noise on high-frequency response spectra. This paper is a companion to Douglas and Boore (2011). In the context of this paper, we describe the motions from the high-sample-rate simulations as the “true” motions. These motions are then high-cut filtered (approximating the anti-alias filter in the recording instrument) and decimated in a process mimicking the digital recording used to obtain ground-motion records similar to those available from various networks, and the PSAs from these modified records are compared with the PSAs from the unmodified (“true”) time series. Deviations of the ratio of PSA (hereafter RRS, for Ratio of Response Spectra) from unity indicate a bias or error in the PSA from the filtered and decimated motions.

As with Douglas and Boore (2011), we find that a critical parameter in judging what error might exist in computing response spectra from the filtered and decimated motions is the ratio of Fourier acceleration spectra (RFAS):

$$RFAS = \frac{FAS(f_{amax})}{FAS(f_{saa})} \quad (1)$$

where  $FAS(f_{amax})$  is the maximum FAS ( $f_{amax}$  is the frequency of the maximum) and  $FAS(f_{saa})$  is the FAS value at the frequency  $f_{saa}$  corresponding to the start of the anti-aliasing filter. The results of Douglas and Boore (2011) are shown in Fig. 1. In their study, various levels of noise were added to simulated spectra, and the RRS were plotted as a function of the RFAS (in this case, the RFAS was computed with a different denominator

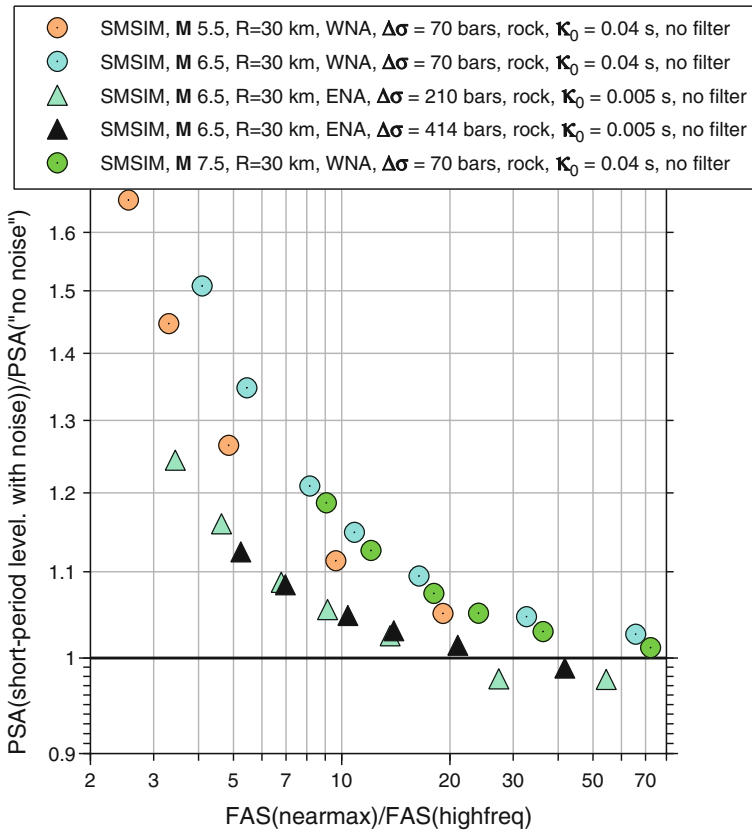


**Fig. 1** Ratios of high-frequency (short-period) response spectra (PSA) from time series with various amounts of added noise with respect to noise-free simulated time series, plotted against the ratios of average Fourier spectra near the peak of the Fourier acceleration spectra (FAS) with respect to the high-frequency noise level. The response spectral ratios correspond to the maximum ratios occurring for frequencies above the frequency at which the FAS noise floor is reached. (Modified from Figure 9 of Douglas and Boore 2011)

than in equation (1): the denominator was the amplitude of the effective floor of the spectrum at high frequencies). As shown in Fig. 1, the error in short-period PSA from ignoring high-frequency noise will be generally less than 15% if the RFAS is greater than a factor of 10.

We also find that the type of resampling of the time series that is part of a common way of computing response spectra can be important, with the usual linear time-domain interpolation leading to response spectra that are generally lower than the true response spectra, even at oscillator frequencies significantly less than  $f_{saa}$ . This bias is largely eliminated by using the Whittaker–Shannon interpolation (Shannon 1998; Wikipedia 2013a). We start with a brief description of the two methods of resampling the acceleration time series when computing response spectra. We follow this with a discussion of the simulation procedure. The results of the simulation study are then presented.

## 2 Effect of interpolation method on response spectral computations

A widely used algorithm for computing response spectra assumes that the acceleration time series is made up of lines connecting the sample points. With this assumption, analytical

equations are used to calculate the oscillator displacement and velocity at one time step in terms of the displacement and velocity at the previous time step (Nigam and Jennings 1969). When the oscillator frequency is such that there are fewer than 10 samples per oscillator period ( $W < 10f_{osc}$ , where  $W$  is the sample rate), it is standard practice to replace the original sampled time series with a time series resampled such that the condition  $W \geq 10f_{osc}$  is met; this resampling assumes that the acceleration is made up of straight lines connecting the original sampled values (e.g., B. Chiou, I. Idriss, and R. Youngs, personal communications, 2010). This resampling is done to obtain a more accurate estimate of the peak response of the oscillator time series.

By definition, an acceleration time series sampled at  $W$  sps should have no energy beyond the Nyquist frequency  $f_{Nyquist}$ , where  $f_{Nyquist} \equiv 0.5W$ . For modern digital recordings, this is assured by the use of hardware anti-aliasing filters applied before analog-to-digital conversion. If the time series is desired at a higher sample rate, the resampling should be done such that no energy is introduced for frequencies beyond  $f_{Nyquist}$  of the original time series. Linear time-domain interpolation of records processed with an anti-aliasing filter to a higher sample rate than the original sample rate violates this condition, and such re-sampled records are expected to lead to errors in the Fourier spectra and response spectra. This issue and the alternative solution described below are discussed in Phillips et al. (2012).

An alternative way to resample the time series is to use the Whittaker–Shannon interpolation (Shannon 1998; Wikipedia 2013a), which involves convolving the original time series with the sinc function  $\sin(\pi t/\Delta t)/(\pi t/\Delta t)$ , where  $t$  is time and  $\Delta t$  is the sample interval ( $\Delta t = 1/W$ ). The sinc interpolation is easily accomplished in the frequency domain, by padding the Fourier spectra beyond the actual Nyquist frequency with zeros, and then transforming back to the time domain (this is done by the program *smc\_interpolate\_time\_series\_using\_fft.for*, part of the TSPP suite of Fortran program [Boore 2013]). We refer to this approach as the “sinc interpolation” method. An alternate that approximates the sinc interpolation is given by Lanczos interpolation (Turkowski and Gabriel 1990; Wikipedia 2013b).

Figure 2 shows a portion of a record originally sampled at 125 sps, filtered to approximate an anti-aliasing filter for a sample rate of  $125 \text{ sps}/3 = 41.67 \text{ sps}$  (the factor of 3 was chosen to give a record whose sample rate is close to the 40 sps rate often encountered in records obtained in CENA). The time series was resampled by connecting the 41.67 sps points with lines (linear interpolation) and by using sinc interpolation (the resampling algorithm we use requires that the new sample rate be a power of two larger than the starting sample rate; in the case shown in Fig. 2, the new sample rate is four times the starting rate). Figures 3 and 4 give the Fourier and response spectra for the various time series in Fig. 2. As shown in Figs. 2 and 3, linear interpolation of a digital acceleration time series can underestimate the absolute peaks in the time series as well as the spectral content for frequencies less than the Nyquist frequency and can introduce high frequencies beyond the Nyquist frequency (due to the discontinuous slopes at the sample points). The sinc interpolation does an excellent job of recovering the original filtered time series. Phillips et al. (2012) contains other examples of sinc interpolation.

### 3 The effect of anti-aliasing filtering on response spectra: method

In order to simulate the recording process that involves anti-aliasing filtering and decimation, and yet have available the “true” ground motion, we could either use real records recorded at sample rates much above those that will be obtained by decimation, or we can use synthetic ground motions computed at a high sample rate. Because it gives more con-

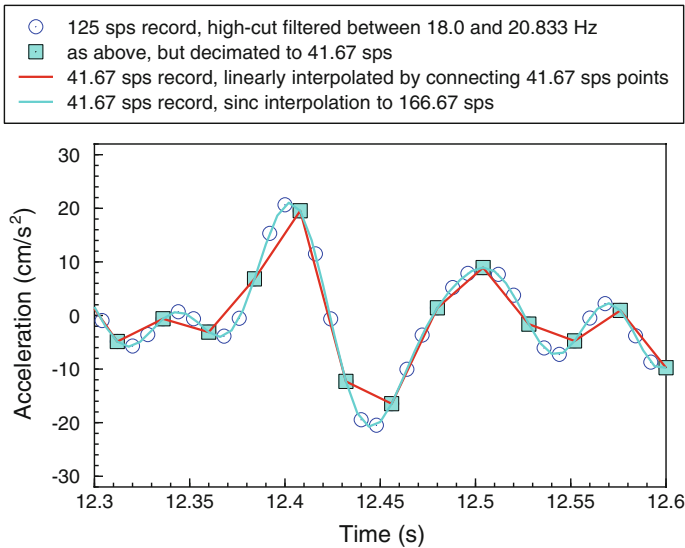


**Fig. 2** A small portion of an accelerogram in the vicinity of the absolute peak amplitude, showing the time series obtained by high-cut filtering a 125 sps time series between 18–20.833 Hz, decimating the filtered time series by a factor of 3 (41.67 sps), and time series from two ways of interpolating the 41.67 sps record to a higher sample rate (no sample rate is shown for the linear interpolation, because that interpolation can provide values at any desired sample rate). The second time series represents the record that would have been obtained by a digital instrument with a sample rate near 40 sps (a sample rate used by many modern instruments recording motions in CENA). Note that the absolute peak amplitude for the sinc interpolation (21.04  $\text{cm/s}^2$  at 12.402 s) is higher than that for the linear interpolation (19.51  $\text{cm/s}^2$  at 12.408 s); this will lead to a difference in pseudo-absolute acceleration spectral response at short periods. The original time series used in this example is the same as used in Figure 3 of Douglas and Boore (2011)

trol over the results, we have primarily used the latter, although we also show results from two real recordings (recorded at 200 sps, for which we simulate 40 and 100 sps records). The synthetic motions were generated using the *a\_ts\_drvr* program in the SMSIM suite of stochastic-method ground-motion simulations programs (Boore 2005). The parameters for the simulations were those of Atkinson and Boore (2006) for eastern North America, except that the source was a single-corner frequency  $\omega^2$  model with a 250 bar stress parameter. Motions were generated for eight input sets sampling two moment magnitudes  $M$  (4.0 and 7.0), two distances  $R$  (5 and 200 km), and two  $\kappa_0$  values (0.005 and 0.050 s), with a sample rate of 1,000 sps (this is a much higher rate than used in practice and was chosen so that the response spectra computed using the usual method would not be subject to any bias for frequencies less than 100 Hz). Ten acceleration time series were generated for each set of  $M$ ,  $R$  and  $\kappa_0$ . Each time series was then filtered and decimated to simulate recordings at 40 and 200 sps. The filter approximated an anti-aliasing filter, with parameters chosen to match the FAS from actual records with sample rates of 40 and 200 sps. The filter was given by a half cycle of a raised cosine, going from unity at  $f = f_{saa}$  to zero at  $f = f_{Nyquist}$ . This filter was easy to implement and judging from its effect on FAS, is a reasonable analog to the actual anti-aliasing filter used in modern recorders. A number of approximations to an anti-aliasing filter were tried; the results of this study are not sensitive to the shape of the filter response between  $f_{saa}$  and  $f_{Nyquist}$ . For the anti-aliasing filters associated with the simulated 40 and 200 sps recordings,  $f_{saa}$  and  $f_{Nyquist}$  were 16 and 20 and 80 and 100 Hz, respectively. Sample FAS for a range of input parameters and

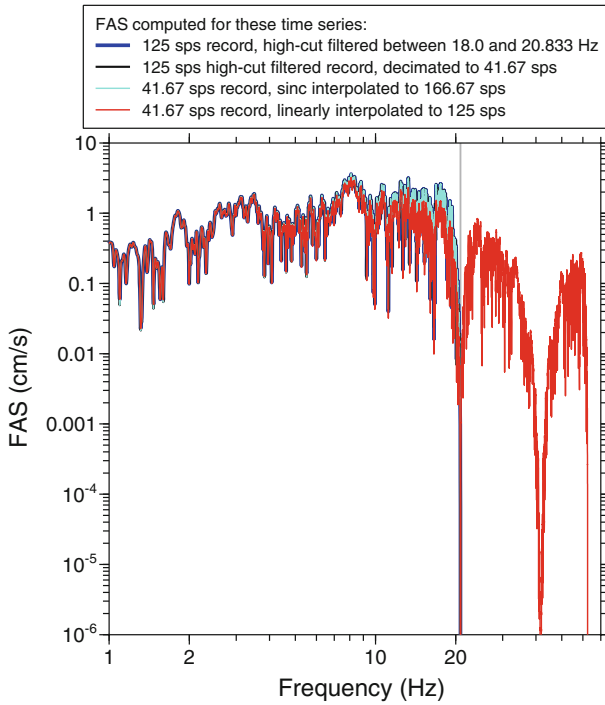


**Fig. 3** The Fourier spectra (FAS) of the time series shown in Fig. 2. The first three curves are almost indistinguishable

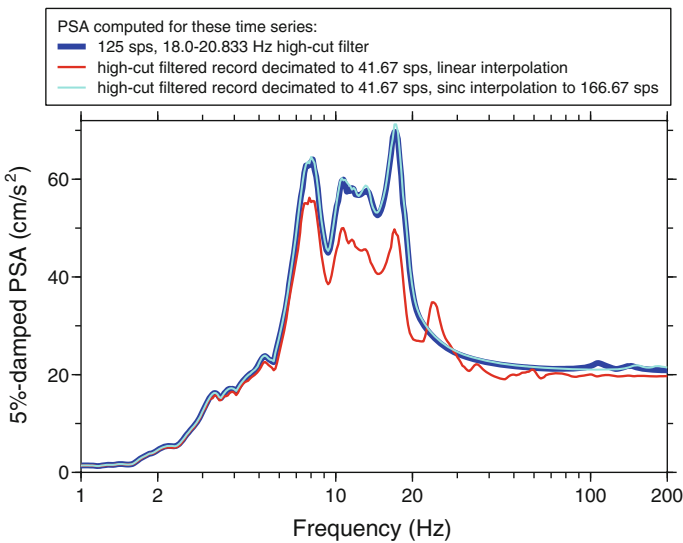


**Fig. 4** The response spectra (PSA) of the time series shown in Fig. 2

filters are shown in Fig. 5. The wide range of range of  $\mathbf{M}$ ,  $\mathbf{R}$ ,  $\kappa_0$ , and  $f_{Nyquist}$  was chosen to obtain a good distribution of RFAS and to see if the results are sensitive to  $\mathbf{M}$ ,  $\mathbf{R}$ ,  $\kappa_0$ , and  $f_{Nyquist}$ .

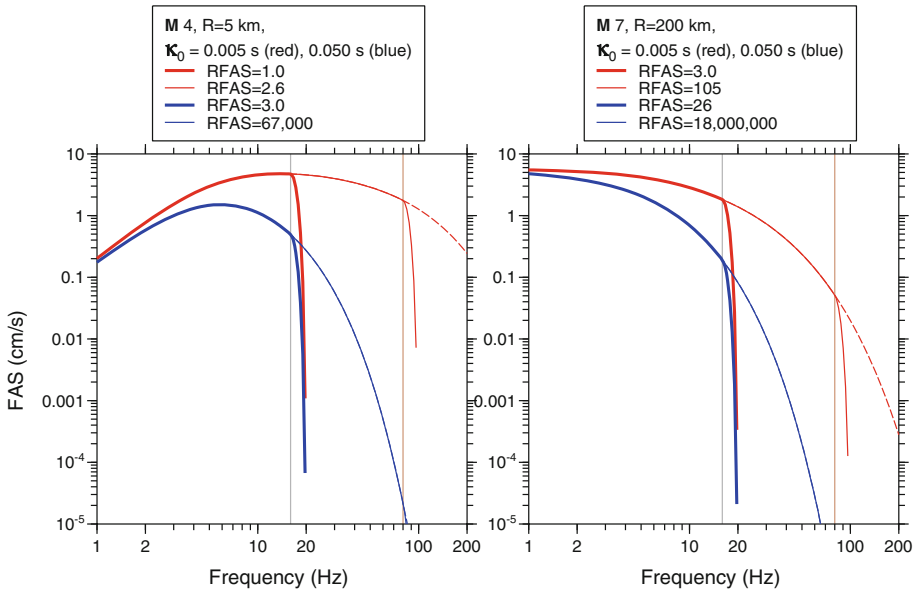


**Fig. 5** Examples of simulated Fourier acceleration spectra (FAS) for a wide range of  $M$ ,  $R$ , and  $\kappa_0$ . The complete set used in this article consists of 16 combinations of  $M$ ,  $R$ , and  $\kappa_0$ :  $M$  4 and 7,  $R=5$  and 200 km,  $\kappa_0 = 0.005$  s and  $\kappa_0 = 0.050$  s, and anti-aliasing filters starting at 16 and 80 Hz (corresponding to simulated time series with Nyquist frequencies of 20 and 100 Hz, respectively). The dashed curves are the simulated FAS before anti-aliasing filtering. The vertical lines are plotted at the start of the anti-aliasing frequencies. The FAS for the two anti-aliasing filters considered in this paper are shown, along with the ratios of the peak FAS (which occurs at the frequency  $f_{max}$ ) to the FAS at the frequency corresponding to the start of the anti-aliasing filter ( $f_{saa}$ )

The simulation procedure yielded 24 sets of 10 acceleration time series, including the unfiltered time series. For each time series, PSA was computed using the interpolation methods described above, and these PSAs were averaged for each set of  $M$ ,  $R$ ,  $\kappa_0$ , and  $f_{Nyquist}$ . The ratios of the average PSA from the filtered and decimated time series with respect to those from the original (“true”) time series provided the basic information from which the conclusions in this article are derived.

#### 4 The effect of anti-aliasing filtering on response spectra: results

The ratios of response spectra are shown for 15 of the 16  $M$ ,  $R$ ,  $\kappa_0$ , and  $f_{Nyquist}$  combinations in Fig. 6. Not shown are the results for  $M$  7,  $R=200$  km,  $\kappa_0 = 0.050$  s, and  $f_{Nyquist} = 100$  Hz, because RFAS is so large ( $10^7$ ) that the response spectral ratios are very close to unity. The curves in Fig. 6 are arranged by the value of RFAS, as indicated in the legend. Note that we use frequency normalized by  $f_{saa}$  for the abscissa, as this brings the ratios from disparate values of  $M$ ,  $R$ ,  $\kappa_0$ , and  $f_{Nyquist}$  together, revealing systematic trends. The comparison of the results from the two methods of resampling clearly show the superiority of the sinc interpolation (top graph) to the linear interpolation (bottom graph) for frequencies less than  $f_{saa}$ . On the other hand, neither method can recover real motion that has been removed by the anti-aliasing filter for frequencies greater than  $f_{saa}$ .

Figures 7 and 8 display the same information as in Fig. 6 in a way that is easier to use in estimating the error that might exist in high-frequency response spectra. These are the

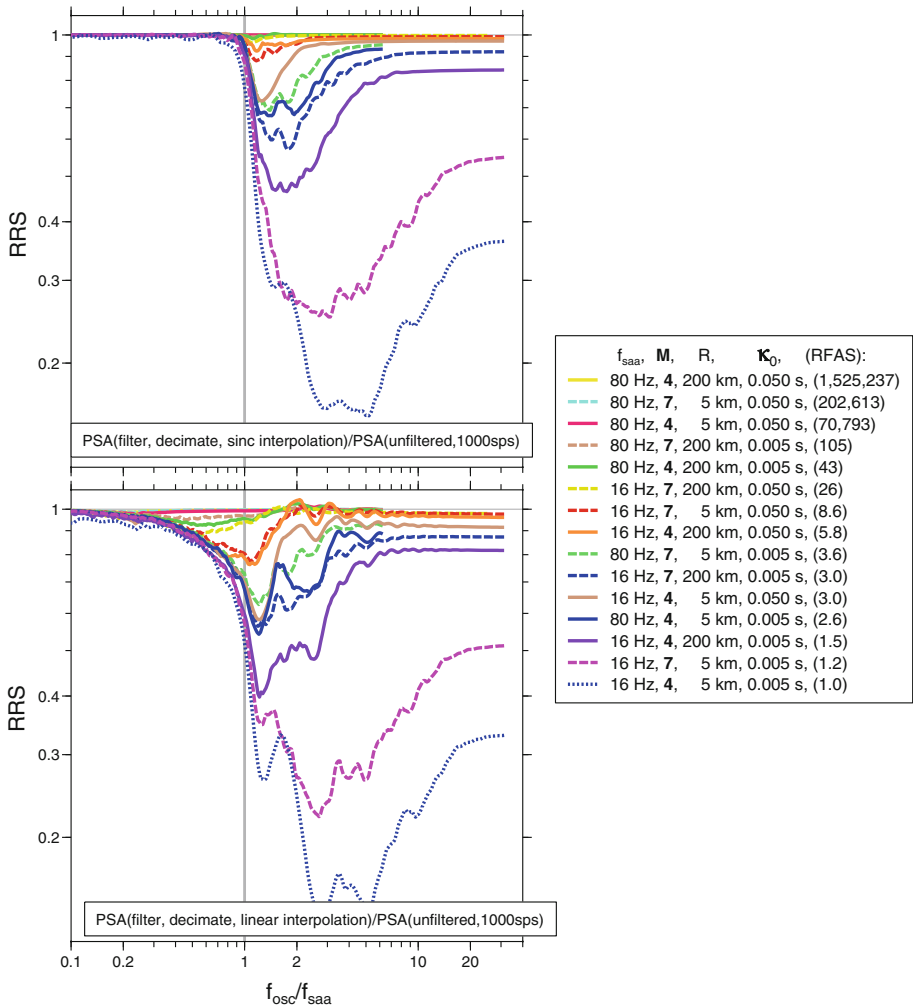


**Fig. 6** Ratios of response spectra (RFAS) for anti-aliased and decimated simulated time series with respect to the response spectra from the simulated time series without filtering and decimation (these spectra correspond to the “true” or “target” spectra). The PSA used in the ratios are the average of the PSA from 10 simulations. The ratios are plotted against oscillator frequency ( $f_{osc}$ ) normalized by the frequency at which the anti-aliasing filter begins ( $f_{saa}$ ). As shown by the legend, the curves represent many combinations of anti-aliasing filters, magnitude, distance, and  $\kappa_0$ ; the curves have been ordered by the RFAS. The *top graph* shows the results when the response spectra computed from the filtered and decimated time series after being resampled to a high sample rate using sinc interpolation. The *bottom graph* shows the results when straight-line interpolation was used to resample the filtered and decimated time series when required by the response spectrum algorithm

key figures for the conclusions reached in this study. Both figures show the ratio of the true response spectrum to that from the filtered and decimated time series (mimicking an actual recording) as a function of the ratio of the FAS at its maximum value ( $f_{amax}$ ) to that at the frequency  $f_{saa}$ . This ratio can be computed for any recording. The symbols are for various values of the normalized oscillator frequency ( $f_{osc}/f_{saa}$ ), with values less than and greater than unity shown in Figs. 7 and 8, respectively.

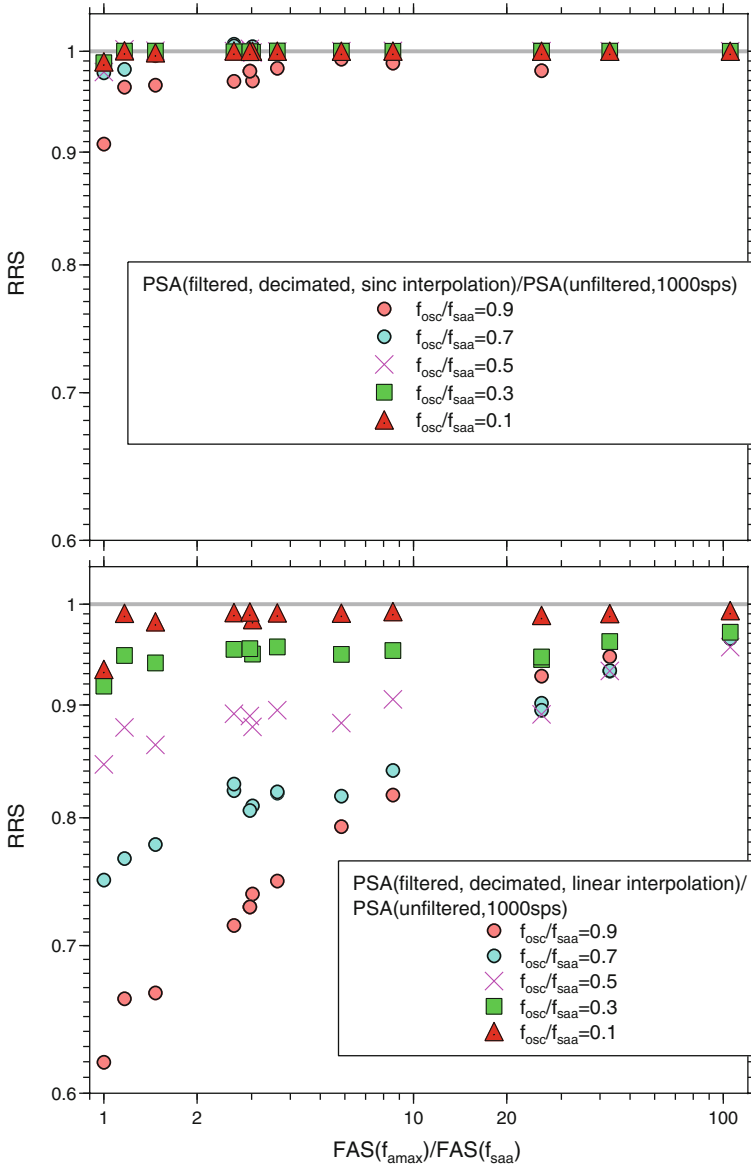


**Fig. 7** Ratio of “true” response spectra (PSA) to the PSA from the filtered and decimated time series used in computing the “true” PSA, plotted against the FAS ratio. The PSA used in the ratios are the average of the PSA from 10 simulations. The results for different values of the normalized frequency are shown by the symbols of different shape and color. This figure only includes normalized frequencies less than unity. The *top graph* shows results in which the PSA were computed from filtered and decimated acceleration time series which were resampled to a high sample rate using sinc interpolation; the PSA in the *bottom graph* were computed from the filtered and decimated acceleration time series resampled using straight-line interpolation when there were fewer than 10 sample points per oscillator period (see text for more discussion). The information in this figure is the same as in Fig. 6, but plotted in a way that makes it easier to estimate the error in the PSA computed using the two resampling methods for a record with a given value of  $FAS(f_{amax})/FAS(f_{saa})$

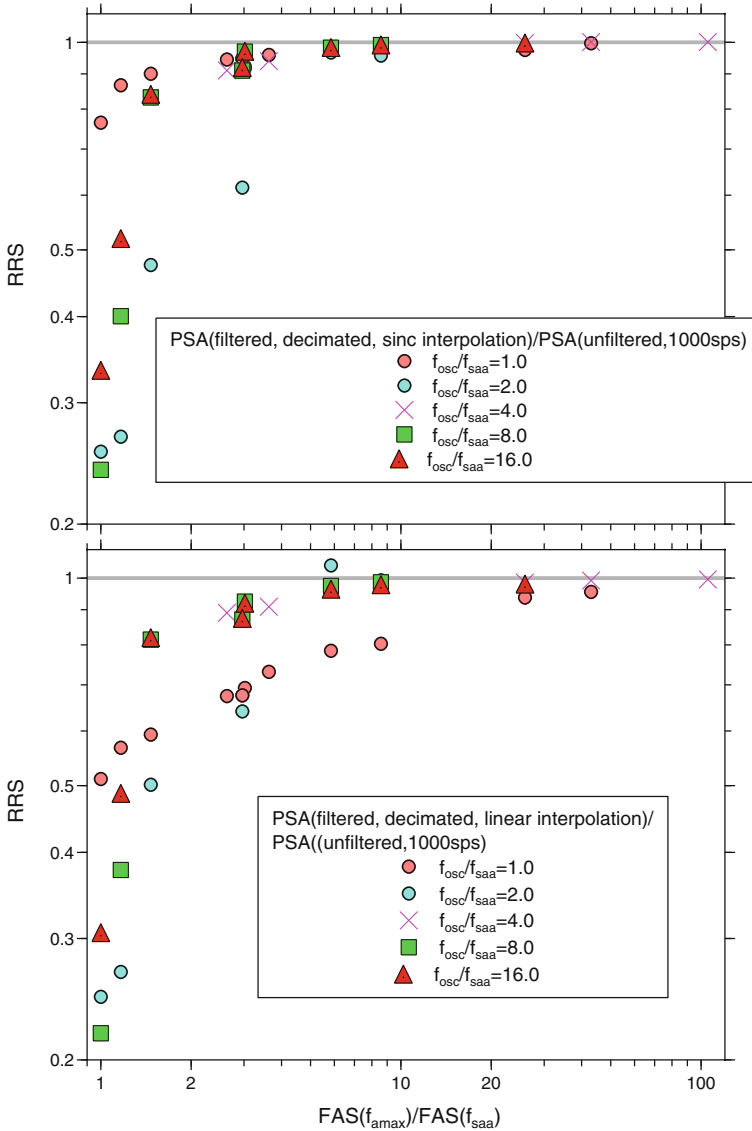


**Fig. 8** Ratio of “true” response spectra (PSA) to the PSA from the filtered and decimated time series used in computing the “true” PSA, plotted against the FAS ratio. The PSA used in the ratios are the average of the PSA from 10 simulations. The results for different values of the normalized frequency are shown by the symbols of different shape and color. This figure only includes normalized frequencies greater than unity. The top graph shows results in which the PSA were computed from filtered and decimated acceleration time series which were resampled to a high sample rate using sinc interpolation; the PSA in the bottom graph were computed from the filtered and decimated acceleration time series resampled using straight-line interpolation when there were fewer than 10 sample points per oscillator period (see text for more discussion). The information in this figure is the same as in Fig. 6, but plotted in a way that makes it easier to estimate the error in the PSA computed using the two resampling methods for a record with a given value of  $FAS(f_{amax})/FAS(f_{saa})$

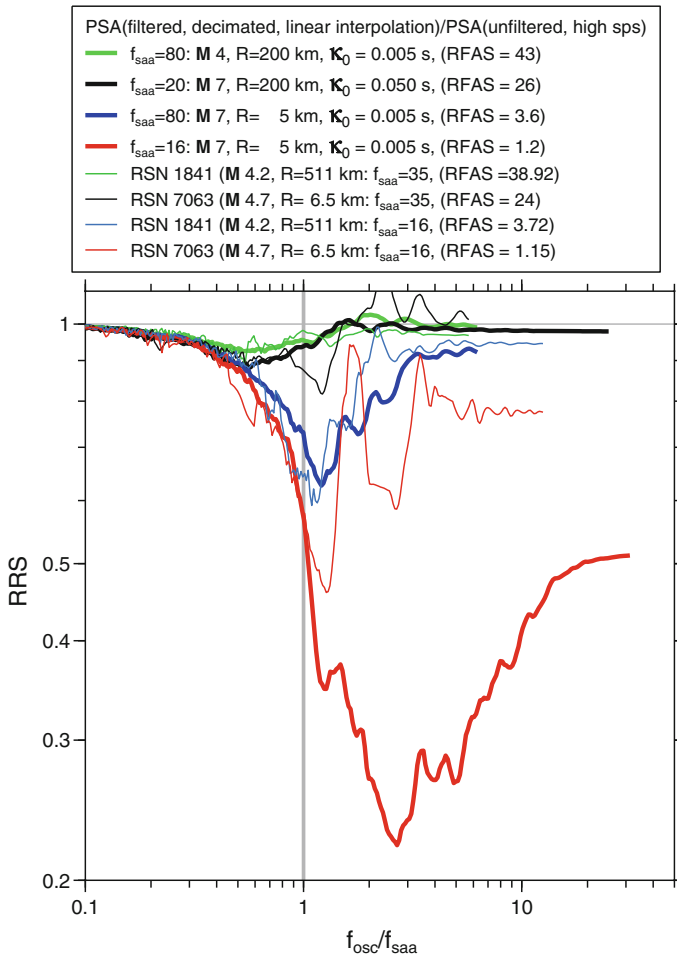
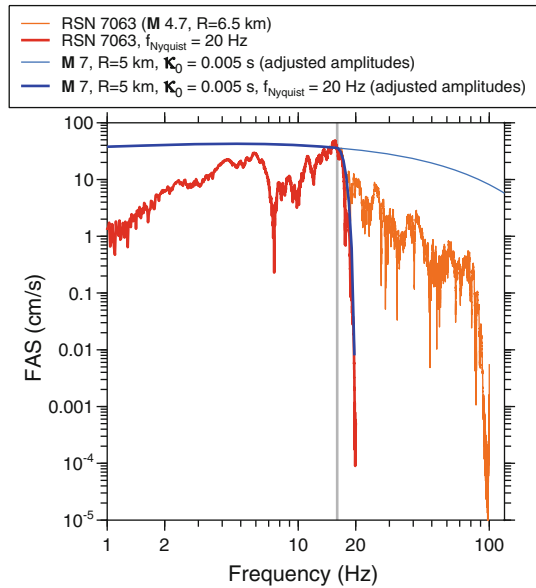


**Fig. 9** Comparison of PSA ratios where both data (sampled at 200sps) and simulations were used in the mimicking the anti-aliasing filter and decimation recording process. The simulated time series were chosen to have values of RFAS similar to those from the observed data. The data records are indicated by their record sequence number (RSN), as used in a forthcoming database being prepared for the PEER NGA-East project. RSN 1841 is from the 01 May 2005 Shady Grove, Arkansas earthquake recorded at station ET.CPCT, and RSN 7063 is from the 28 February 2011 Greenbrier, Arkansas earthquake recorded at station NM.X301. The preliminary estimates of  $V_{S30}$  for these stations is around 430 m/s

Figure 7 indicates that there will be little error in the PSA values for oscillator frequencies less than  $f_{saa}$  for any value of RFAS when sinc interpolation is used to resample the time series before computing the response spectrum. This is the first of the two main conclusions of this article. In contrast, the error in the PSA computed using linear interpolation for the resampling can be substantial, growing as the oscillator frequency approaches  $f_{saa}$  and as RFAS decreases. Even for RFAS=10, the error can be about 20 % for a frequency as low as  $0.7f_{saa}$ , with even larger errors for frequencies closer to  $f_{saa}$ .

When the oscillator frequency exceeds  $f_{saa}$ , Fig. 8 shows that both interpolation methods result in significant underestimation of the “true” PSA when RFAS is small—this is simply because a significant amount of high-frequency energy has been removed by the anti-aliasing

**Fig. 10** Comparison of Fourier acceleration spectra (FAS) from the observed data (RSN 7063) and simulated data. The *thin lines* are the FAS as recorded and simulated, and the *thick lines* are the FAS after anti-aliasing filtering (in this example the time series was not decimated before the FAS was computed). The FAS for the simulations were adjusted vertically to have the same peak amplitude as the FAS from the observed data. The *vertical gray line* shows the start of the anti-aliasing filter (a raised cosine between 16 and 20 Hz). Both FAS have the same ratio of the peak to that at the start of the anti-aliasing filter ( $RFAS = 1.2$ )



filter. The sinc interpolation is marginally better, as RRS approaches unity for smaller values of  $RFAS$  for oscillator frequencies close to  $f_{saa}$ . In general, however, the error will be less than 10% when  $RFAS$  exceeds a factor of 10. This is the second of the two main conclusions of this article.

We repeated the process by filtering and decimating several real records from CENA which were originally sampled at 200 sps. The RRS from the filtered and decimated time series with respect to the PSA from the original data are compared to results from synthetic data in Fig. 9, where the synthetic data were chosen with  $RFAS$  similar to those from the real data. In order to show more detail for  $f_{osc}/f_{saa} < 1$ , only results using linear interpolation resampling are shown in Fig. 9 (the ratios from the sinc interpolation for  $f_{osc}/f_{saa} < 1$  are close to unity). For similar values of  $RFAS$  the results from the simulated and real data are comparable, with one exception: for the smallest value of  $RFAS$  (1.2), the PSA ratio is much smaller for the synthetic data than for the real data for oscillator frequencies greater than  $f_{saa}$ .

The reason for the difference in RRS for small values of  $RFAS$  is instructive. Figure 10 shows the FAS of the observed and synthetic data, before and after filtering with the 16–20 Hz anti-aliasing filter. The FAS for the synthetic data have been adjusted to go through the maximum of the FAS from the observed data. Both FAS have approximately the same value of  $RFAS$  (1.2). The FAS of the unfiltered synthetic data decays much less rapidly, however, than that from the observed data. For this reason, more energy that would have contributed to the high-frequency PSA (if recorded at a high sample rate) is lost through the anti-aliasing filter for the synthetic data than for the observed data, leading to a larger difference in RRS for the synthetic data than for the observed data. The implication is that the actual error in the high-frequency PSA for digital recordings could be less than estimated from the simulations (Fig. 8) because the FAS from true ground motions might decay more rapidly beyond the decimated motion’s Nyquist frequency than the FAS from the simulations. (As indicated in the legend in Fig. 6, the smallest values of the FAS ratio from the simulated data are associated with  $\kappa_0 = 0.005$  s, for which FAS decay slowly at close distance. This value of  $\kappa_0$  is commonly used for recordings on very hard rock, but in many cases, such as that for the sites that provided the data used in the figure, we expect that the  $\kappa_0$  values could even

be larger.) What would be needed to give a more accurate estimation of the error in high-frequency PSA is not just the ratio of the maximum value of the FAS to the value at  $f_{saa}$ , but also the high-frequency content of the ground motion before filtering and decimation. This, however, is essentially unknowable. The simple FAS ratio will give an estimate of the maximum error, which is useful in defining the usable PSA bandwidth.

## 5 Conclusion

Simulations of modern digital ground-motion recorders using synthetic acceleration time series as input to the recorders were made in order to assess the error in high-frequency pseudo-response spectral acceleration (PSA) at oscillator frequencies above the start of the anti-aliasing filters used in the recordings. As in a complementary study of the effect of noise on high-frequency response spectra by Douglas and Boore (2011), we find that a key parameter in assessing the potential error in high-frequency PSA is the ratio of the Fourier acceleration spectrum near its maximum value to that at the frequency corresponding to the start of the anti-aliasing filter  $f_{saa}$ . As also found by Douglas and Boore (2011), if the FAS ratio is greater than about 10, then the response spectra at frequencies above the anti-aliasing filter should be close to that of the actual ground motion (unaffected by the filtering and decimation associated with digital recording). This conclusion should apply no matter whether the FAS at high frequencies is dominated by signal or noise, because in either case the FAS at high frequencies will be small enough relative to the peak of the FAS that the high-frequency response spectrum will be controlled by ground-motion frequencies less than the frequency of the anti-aliasing filter. If the FAS ratio is less than about a factor of 10, the high-frequency PSA might not have much error if the actual ground motion had little high frequency content to begin with. But this is essentially unknowable from the recorded data, and therefore response spectra for frequencies greater than the anti-aliasing filter frequency should be used with caution if the FAS ratio is less than about 10.

A second conclusion has to do with the resampling of the digital acceleration time series that is part of the commonly used Nigam and Jennings (1969) algorithm for computing response spectra: it is better to use sinc interpolation than the usual linear interpolation, as that gives a better estimates of the peak motions, reproduces the acceleration waveforms more accurately, does not underestimate the motion near the anti-aliasing corner frequency and does not introduce spurious energy at high frequencies. While this conclusion may be obvious to experts in digital signal processing, it is our experience that it is not appreciated by those involved with the processing and use of earthquake ground motions for engineering purposes. The state-of-practice is to use linear interpolation.

**Acknowledgments** This study was sponsored by the Pacific Earthquake Engineering Research Center (PEER) as part of NGA-East, a project funded by the U.S. Nuclear Regulatory Commission (NRC), the U.S. Department of Energy (DOE) and the Electric Power Research Institute (EPRI), with the participation of the U.S. Geological Survey (USGS). Any opinions, findings, and conclusions or recommendations expressed in this material are those of the authors and do not necessarily reflect those of the organizations listed above. We thank Norm Abrahamson for making us aware of possible inaccuracies in response spectra computed from low sample rate data using the standard programs for the computations and for suggesting a solution to the problem. We also thank Albert Kottke for his input early on and for alerting us to the Phillips et al. (2012) paper, and Rasool Anooshehpour, Robert Darragh, John Douglas, and an anonymous person for reviews of the manuscript.

## References

- Anderson JG, Hough SE (1984) A model for the shape of the Fourier amplitude spectrum of acceleration at high frequencies. *Bull Seismol Soc Am* 74:1969–1993
- Atkinson GM, Boore DM (2006) Earthquake ground-motion prediction equations for eastern North America. *Bull Seismol Soc Am* 96:2181–2205
- Boore DM (2005) SMSIM—Fortran programs for simulating ground motions from earthquakes: version 2.3—A revision of OFR 96–80-A, U.S. Geological Survey open-file report, U.S. Geological Survey open-file report 00–509, revised 15 Aug 2005, p 55. The latest version of the software (v. 4.0, as of 11 Oct 2013) is available from the online software link on <http://www.daveboore.com>
- Boore DM (2013) TSPP—A collection of FORTRAN programs for processing and manipulating time series, U.S. Geological Survey open-file report 2008-1111 (Revision 4.4). Available from the online software link on <http://www.daveboore.com>
- Douglas J, Boore DM (2011) High-frequency filtering of strong-motion records. *Bull Earthq Eng* 9:395–409
- Nigam NC, Jennings PC (1969) Calculation of response spectra from strong-motion earthquake records. *Bull Seismol Soc Am* 59:909–922
- Phillips C, Kottke AR, Hashash YMA, Rathje EM (2012) Significance of ground motion time step in one dimensional site response analysis. *Soil Dyn Earthq Eng* 43:202–217
- Shannon CE (1998) Communication in the presence of noise (a reprint of the classic 1949 paper). *Proc IEEE* 86:447–457
- Silva WJ, Darragh RB (1995) Engineering characterization of strong ground motion recorded at rock sites. Electric Power Research Institute, Palo Alto, CA. Report No. TR-102262
- Turkowsky K, Gabriel S (1990) Filters for common resampling tasks. In: Glassner AS (ed) *Graphics gems I*. Academic Press, Waltham, pp 147–165
- Wikipedia (2013a) Whittaker–Shannon interpolation formula. [http://en.wikipedia.org/wiki/Whittaker-Shannon\\_interpolation\\_formula](http://en.wikipedia.org/wiki/Whittaker-Shannon_interpolation_formula). Accessed 09 Oct 2013
- Wikipedia (2013b) Lanczos sampling. [http://en.wikipedia.org/wiki/Lanczos\\_resampling](http://en.wikipedia.org/wiki/Lanczos_resampling). Accessed 09 Oct 2013